




Cell-specific gene therapy driven by an optimized hypoxia-regulated vector reduces choroidal neovascularization

Manas R. Biswal^{1,2} · Howard M. Prentice^{3,4}  · George W. Smith¹ · Ping Zhu⁵ · Yao Tong² · C. Kathleen Dorey⁶ · Alfred S. Lewin² · Janet C. Blanks^{1,4}

Received: 28 December 2017 / Revised: 31 July 2018 / Accepted: 6 August 2018 / Published online: 13 August 2018
© Springer-Verlag GmbH Germany, part of Springer Nature 2018

Abstract

Aberrant growth of blood vessels in the choroid layer of the eye, termed choroidal neovascularization (CNV), is the pathological hallmark of exudative age-related macular degeneration (AMD), causing irreversible blindness among the elderly. Co-localization of proangiogenic factors and hypoxia inducible factors (HIF) in neovascular membranes from AMD eyes suggests the role of hypoxia in pathogenesis of CNV. In order to utilize hypoxic conditions in RPE for therapeutic purposes, we developed an optimized hypoxia regulated, RPE cell-specific gene therapy to inhibit choroidal neovascularization. An adeno-associated virus (AAV2) vector comprising a RPE-specific promoter and HIF-1 response elements (HRE) was designed to regulate production of human endostatin (a powerful angiostatic protein) in RPE. The vector was tested in a mouse model of laser-induced CNV using subretinal delivery. Spectral domain optical coherence tomography (SD-OCT) images from live mice and confocal images from lectin stained RPE flat mount sections demonstrated reduction in CNV areas by 80% compared to untreated eyes. Quantitative real-time polymerase chain reaction (qPCR) confirmed exogenous endostatin mRNA expression from the regulated vector that was significantly elevated 3, 7, and 14 days following laser treatment, but its expression was completely shut off after 45 days. Thus, RPE-specific, hypoxia-regulated delivery of anti-angiogenic proteins could be a valuable therapeutic approach to treat neovascular AMD at the time and in the ocular space where it arises.

Key points

- An optimized gene therapy vector targeting hypoxia and tissue-specific expression has been designed.
- The inhibitory role of gene therapy vector was tested in a mouse model of laser-induced CNV.
- An 80% reduction in choroidal neovascularization was achieved by the optimized vector.
- The expression of endostatin was limited to retinal pigment epithelium and regulated by hypoxia.

Keywords Choroidal neovascularization · Retinal pigment epithelium · Hypoxia responsive element · Endostatin · Adeno-associated virus · Gene therapy · Age-related macular degeneration

Manas R. Biswal and Howard M. Prentice contributed equally to this work.

Preliminary data were presented in abstract form at The Association for Research in Vision and Ophthalmology (ARVO) annual conference, 2010 Fort Lauderdale, FL (USA) and Retinal Degeneration Symposium 2010, Mt. Tremblant, CAN

✉ Howard M. Prentice
hprentic@health.fau.edu

¹ Integrative Biology Program, Dept. of Biology, Florida Atlantic University, Boca Raton, FL, USA

² Department of Molecular Genetics and Microbiology, University of Florida College of Medicine, Gainesville, FL, USA

³ Charles E. Schmidt College of Medicine, Florida Atlantic University, 777 Glades Road, Boca Raton, FL 33431, USA

⁴ Center for Complex Systems and Brain Sciences, Florida Atlantic University, Boca Raton, FL, USA

⁵ Department of Ophthalmology, University of Florida College of Medicine, Gainesville, FL, USA

⁶ Virginia Tech Carilion School of Medicine, Roanoke, VA, USA

Introduction

Age-related macular degeneration (AMD) is the most common cause of irreversible vision loss among older populations in the industrialized world [1, 2]. AMD exhibits two clinical subtypes: the slower dry form with foci of progressive death of retinal pigment epithelium (RPE) and photoreceptors and the rapidly forming wet form characterized by choroidal neovascularization (CNV), both ultimately causing significant photoreceptor cell degeneration [3]. The neovascular form occurs in 15% of all AMD patients, and 80% of these have severe vision loss [4]. Choroidal neovascularization (CNV) occurs in response to proangiogenic factors like vascular endothelial growth factor (VEGF) in which new vessels grow from choroidal capillaries through aged and thickened Bruch's membrane into the sub-RPE space and often into the retinal layers. Co-localization of VEGF and hypoxia inducible factors (HIF) in neovascular membranes from eyes with AMD suggests the role of hypoxia in developing physiologic and pathophysiologic conditions of AMD [5].

Being a potent angiogenic factor, VEGF plays an important role in development of CNV [6]. Most current therapies targeting CNV use intravitreal delivery of anti-angiogenic (mostly VEGF inhibitors) or anti-inflammatory agents alone or in combination with photodynamic therapy and radiation [7]. The VEGF blocking drugs (bevacizumab, ranibizumab, aflibercept) are effective in slowing the rate of vision loss in patients with wet AMD and improve vision in a significant number of patients. However, these treatments are short-lived and require repeated and expensive intra-ocular injections and are associated with risk for rare intravitreal infections or retinal alteration due to deprivation of VEGF, a neuronal survival factor [8, 9].

Ocular gene therapy delivering anti-angiogenic agents could avoid repeated injections but VEGF-A has a potential neuroprotective role in the retina, so that long-term suppression may be problematic [10].

Regulation of the transgene avoids these potential problems and offers rapid targeting of recurrence of CNV, a common clinical problem. Therefore, there is a need for a long-term, regulated, and cost-effective therapeutic option to treat wet AMD. With this goal in mind, we developed an optimized gene therapy platform based on a tightly regulated gene promoter that exploits the pathological retinal condition of hypoxia to drive expression of a therapeutic gene product.

Expression of VEGF is intrinsically regulated by the transcription factor hypoxia inducible factor-1 (HIF-1), which is activated in response to hypoxia, inflammation, and oxidative stress and which binds to hypoxia response elements (HREs) to regulate target genes [11–13]. HIF-1 levels are increased in CNV lesions from both AMD patients and experimental animal models [5, 14] where targeting HIF-1 reduces neovascularization and VEGF secretion [15–17]. We previously

reported the effectiveness of HRE elements to drive RPE-[18] and Müller-cell-specific reporter gene expression in hypoxia [19].

Endostatin, a 20-kDa proteolytic fragment of the carboxyl terminus of collagen XVIII [20], is an angiostatic agent that significantly reduces experimentally induced CNV [21]. We recently reported that a novel hypoxia-regulated, glial cell-specific vector for expression of endostatin significantly reduced retinal neovascularization in response to physiological hypoxia [22]. Viral-mediated delivery of constitutively expressed endostatin has been tested in mouse models of retinopathy of prematurity [23] as well as a model of experimental CNV [24]. Recently, a safety study of a lentiviral vector based on equine infectious anemia virus (EIAV) delivering endostatin for treatment of wet AMD was reported [25]. In these patients, gene delivery of endostatin was well tolerated but no significant change in lesion size was observed.

Our study tested the hypothesis that a hypoxia-regulated, RPE-specific vector would deliver a sufficient quantity of anti-angiogenic endostatin to significantly reduce laser-induced CNV. Our results demonstrated that pretreatment with this hypoxia-regulated, RPE-specific vector successfully reduced CNV in mice. Not only is this gene expression regulated by the hypoxic conditions of the pathological retina, but it is also specific to the RPE cells, so therapy will be targeted to the appropriate area (RPE-choroid) to treat neovascular AMD.

Methods

Vector construction and packaging

The HRSE-6XHRE-RPE65 promoter assembly in a pGL3 basic vector has been previously outlined [18]. Construction of the hypoxia-regulated endostatin plasmid vector is described in Fig. 1. Briefly, the human endostatin XVIII cDNA plus an SV40 polyadenylation signal was PCR-amplified from pBLAST42-hEndo XVIII plasmid (InvivoGen, San Diego, CA) and then subcloned in a self-complementary AAV serotype 2 (AAV-2) plasmid to produce scAAV2-CMV-hEndostatin (scAAV2-CMV-Endo). The HRSE-6xHRE-RPE65 promoter [18] was PCR amplified and cloned into scAAV2-REG-GFAP-hEndostatin-FLAG plasmid [22] replacing the REG-GFAP promoter to produce scAAV2-HRSE-6xHRE-RPE65-hEndostatin-FLAG plasmid (REG-RPE-ENDO). The hypoxia-restricted silencing element (HRSE) is composed of three copies of the neuron-restricted silencing element (NRSE) and three copies of the hypoxia-responsive element (HRE). The NRSE (S) and HRE (H) are located in alternating tandem order and form the HRSE which is silent in normoxia but activated at high level in hypoxia [18]. The scAAV2 serotype 2 viral vectors were produced at the University of North Carolina (UNC) Vector Core facility

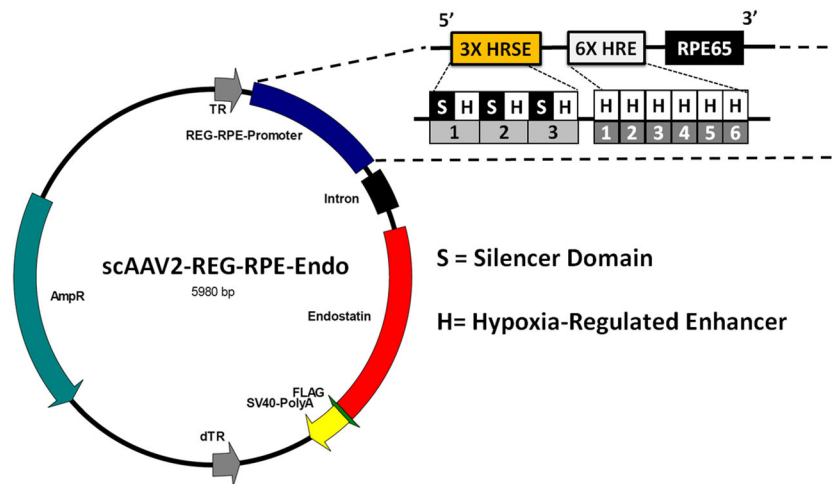


Fig. 1 Vector design. AAV plasmid was used to clone human endostatin cDNA driven by the promoter region of RPE65 gene and hypoxia-regulated elements (HREs). HRSE-6XHRE-RPE65 promoter has been taken from the previously published construct [18]. The promoter with the HREs is termed REG-RPE. The regulated endostatin construct contains the tandem alternating repeats of three copies of NRSE silencer elements (S) with three copies of HRE HIF-1 enhancer elements (H) upstream of the RPE65 promoter, as well as six more

tandem copies of the HRE HIF-1 enhancer element downstream of the HRSE silencer. The silencing domain within the HRSE restricts gene expression only to hypoxia whereas RPE65 promoter permits RPE-specific gene expression. The *Rpe65* promoter (−325 to +52) was derived from the 5′ upstream sequence of the mouse *Rpe65* gene (a generous gift from Dr. Michael Redmond) [26]. The human endostatin cDNA with 3′ flag tag has been cloned to the 3′ end of the promoter to detect exogenous endostatin expression

(Chapel Hill, NC) and the University of Florida’s Ophthalmology Gene Therapy Vector Core facility (Gainesville, FL) respectively. Control vector CMV-GFP is self-complementary CMV-GFP adeno-associated virus serotype 2 from UNC Vector Core Facility.

Animals

Animal experiments employed C57BL/6 mice (aged 7 to 9 months) and were conducted in accordance with the policies of FAU IACUC, University of Miami IACUC, and University of Florida IACUC.

Vector delivery

The trans-corneal method for subretinal injection was used to deliver AAV vectors [27]. Pupils were dilated twice with one drop each of phenylephrine hydrochloride (2.5%) (Paragon Biotech, Portland, OR) and Atropin Sulfate (1%) (AKORN, Lake Forest, IL) at 30-min intervals prior to anesthesia. The mice were anesthetized by intraperitoneal administration of ketamine (80 mg/kg body weight) and xylazine (10 mg/kg body weight) mixture. Prior to subretinal injection, a drop of local anesthesia (proparacaine) and a drop of hypromellose ophthalmic demulcent solution (2.5%) (GONAK™) (AKORN) were applied to the ocular surface. Using a 30 gauge pointed needle, a pilot hole was made at nasal corneal border. For subretinal injection, 1 μ l of virus (at 1.0×10^{12} virus molecules/ml) or vehicle [phosphate-buffered saline (PBS)] was gently delivered below the retina using a 33 gauge

blunt-ended needle on a Hamilton syringe. We performed one injection per eye with CMV-ENDO or REG-RPE-ENDO while the contralateral eye was injected with vehicle. The unregulated CMV-ENDO vector was selected to measure suppression of CNV with an unregulated promoter with high activity. Successful injections were noted upon fundus visualization of subretinal blebs, indicating retinal detachment that was typically transient and resolved within 24 h. “No Laser” controls were performed by subretinal injection, but without any laser treatment.

SD-OCT: spectral domain coherence tomography

Two weeks following subretinal injection, spectral domain optical coherence tomography (SD-OCT) was employed to visualize any sustained detachment resulting from subretinal injection [28]. The injected eyes were dilated and the mice were anesthetized as described above for subretinal injection. One thousand linear B-scans and 100 images were taken using an Envisu ultra high-resolution instrument (Biotigen, Research Triangle Park, NC) and these images were averaged. Mice showing detachment or retinal damage were eliminated from further studies and euthanized according to approved protocols.

Mouse model of choroidal neovascularization

The laser-induced murine model of CNV has been previously described [29, 30]. Either a vector or vehicle was first introduced by subretinal injection into the retina. The retina was

subsequently treated with a laser at 14 days, 21 days, or 120 days after subretinal injection as specified in results and figure legends. For laser treatment, pupils were dilated and mice were anesthetized. CNV was induced with an argon 532-nm green diode laser (100- μm spot size, 150-mW intensity, 0.1-s duration—Nidek GYC-1000, Fremont, CA) mounted on a Haag-Streit slit lamp, using a handheld coverslip as a contact lens. Three lesions were made at 3, 6, and 9 o'clock positions of the posterior pole of the retina, 2–3 disc diameters away from the optic nerve and avoiding major vessels. Formation of a bubble at the time of laser application indicated rupture of Bruch's membrane and only lesions that produced a bubble were included in this study.

Fundus imaging

A fundus imaging system (Micron III; Phoenix Research Labs, Pleasanton, CA) was used to image the retinas in living mice following laser treatment [31]. Mice were anesthetized and images were taken to locate the laser spots around optic nerve. The eyes showing changes in retinal integrity were eliminated from further studies.

Endostatin ELISA

Endostatin concentrations in the choroid/RPE/retina were measured using a human endostatin ELISA kit (Ray Biotech, Inc., Norcross, GA). Following euthanasia and eye removal eye cups lacking cornea and lens were sonicated in PBS, and the supernatant was collected to measure levels of endostatin produced as previously described [22].

Real-time quantitative PCR

Expression of endostatin was measured using real-time quantitative PCR. Animals were subjected to laser treatment at 21 days or 120 days after subretinal injection of vector. Eyes were collected 3 days, 7 days, 14 days, and 45 days after laser treatment, RPE/choroid was collected, RNA was isolated, and cDNA was prepared using iScript™ cDNA synthesis kit from Bio-Rad (Hercules, CA). Primers employed for human endostatin mRNA quantification by qRT-PCR were forward: GGCTGACCGAGAGCTACTGT and reverse: CATCCTTGTAAATCACGCGTCT. The primers were carefully validated and employed for real-time PCR with relative gene expression being quantified by comparison to mRNA levels for the housekeeping gene encoding GAPDH.

RPE/choroid flat mounts

Fourteen days post-laser mice were anesthetized and the vasculature was stained by cardiac perfusion with 100 μl of 1 mg/ml of tomato lectin conjugated with fluorescein or DyLight

594 (Vector Laboratories, Burlingame, CA) in PBS. Five minutes later, mice were euthanized in 100% CO_2 ; the eyes enucleated and the cornea pierced prior to fixation for 1 h in 4% paraformaldehyde. The RPE, choroid, and scleral complex were carefully dissected, flat mounted on a slide, and coverslipped using Vectashield containing DAPI counterstain (Vector Laboratories, Burlingame, CA). RPE flat mount was imaged using a Leica SP5 confocal microscope (Leica Microsystems, Wetzlar, Germany) equipped with LAS software for compressed 20- μm Z-stack images (1 $\mu\text{m}/\text{frame}$).

Analysis of choroidal neovascularization from RPE/choroid flat mounts

CNV areas were determined by measuring areas of lectin stained vessels surrounding each laser lesion [21]. CNV areas were quantified using ImageJ (<https://imagej.nih.gov/ij/>). The initial number of CNV lesions associated with bubble formation upon laser application was 331 (138 vehicle treated, 169 REG-RPE-ENDO treated, and 24 CMV-ENDO treated). Exclusion and inclusion criteria for CNV lesions and area measurements were developed, then implemented by an investigator who did not know the identity of the treatment groups. Only lesions in eyes that exhibited a retinal bleb after vector injection and that also formed a bubble after laser application were included in analysis. Any lesions associated with retinal bleeding or poor microscopic documentation were excluded from analysis. The individual Z-stacked images (20 μm) of lesions from vehicle-, REG-RPE-ENDO-, and CMV-ENDO-treated eyes were compressed for further analysis. Three lesions from each eye were selected and each lesion was measured three times.

Analysis of choroidal neovascularization from SD-OCT images

A simple optical coherence tomography (OCT) quantification method was used to compare choroidal neovascularization [32]. Fourteen days after laser treatment, high-resolution SD-OCT images were produced as described above from randomly selected mice within each treatment group. The volume of isolated lesions in each eye was quantified as ellipsoids using the formula $[(4/3)\pi(a/2)(b/2)(c/2)] = [(\pi/6)abc]$. In this case, width (a) and depth (b) of the lesion were measured from B-scan images. The distance between the beginning and the end of lesion in the *en face* image was calculated as the length (c).

Immunolocalization of endostatin

For experiments involving immunolocalization of endostatin, REG-RPE-ENDO, CMV-ENDO, or vehicle was delivered by subretinal injection as described above, and then laser injury was carried out 14 days later. Six eyes were analyzed for each

experimental condition. Serial cryosections (8 μm) of formaldehyde-fixed eyes were harvested 3 days post-laser injury and mounted on poly-lysine-coated slides. After washing in PBS, sections were blocked for 2 h and then incubated overnight at 4 $^{\circ}\text{C}$ in primary antibody (goat anti-human endostatin; 1:100, R&D Systems, Minneapolis, MN, in blocking buffer). After washing and then incubation in donkey anti-goat-Alexa-488 (1:1000, Molecular Probes, Eugene, OR) for 2 h at room temperature, slides were washed, air-dried, and coverslipped and then imaged on a Nikon Eclipse TE2000-S inverted fluorescent microscope (Nikon Instruments Inc., Melville, NY).

Statistical analysis

Results were presented as mean \pm SEM. Significance was determined using analysis of variance with Newman-Keuls multiple comparison test. Differences between conditions were regarded as significant if $P < 0.05$. The statistical significance between two groups was analyzed by unpaired two tailed t test and considered significant if $P < 0.05$.

Results

Subretinal injection of REG-RPE-ENDO reduces laser-induced CNV

A CMV-GFP vector (scAAV-CMV-GFP) was used to verify transduction efficiency prior to use of the endostatin vectors. Using the trans-corneal method for subretinal injection [33], we consistently observed nearly 100% of RPE transduction 3 weeks after injection of 1 μl containing 1.0×10^9 vector genome particles (vgp), (data not shown). We compared the CNV response of eyes injected with CMV-ENDO and those injected with REG-RPE-ENDO (1.0×10^9 vgp each), with vehicle-injected eyes. Fourteen days after subretinal injection of vectors or vehicle, laser lesions were created as described above. A further 2 weeks after retinal laser treatment, mice were perfused with fluorescently labeled tomato lectin and flat mount preparations of RPE/choroid complexes were prepared for analysis.

Confocal images on flat mounts showed that lesions from vehicle-injected eyes were visibly larger and had more tortuous vessels than those from either group of endostatin vector-injected eyes (Fig. 2). In each mouse injected unilaterally with REG-RPE-ENDO, we compared the CNV area of the vector-treated eye with that of the vehicle-injected eye. There was a reduction in CNV area in the treated eye in every case (Fig. 3a). Figure 3b shows the volume of CNV in eyes injected with REG-RPE-ENDO by comparison to the contralateral vehicle-injected eyes. These data clearly show a significant 80% decrease in CNV ($P < 0.001$) resulting from the use of

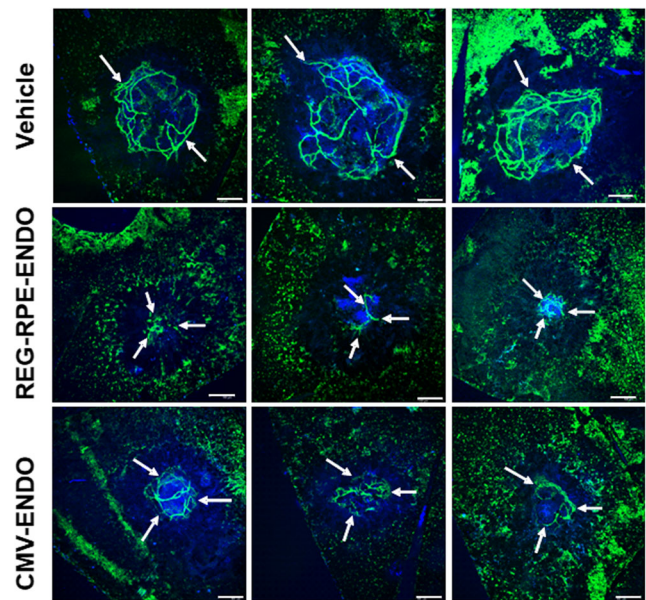


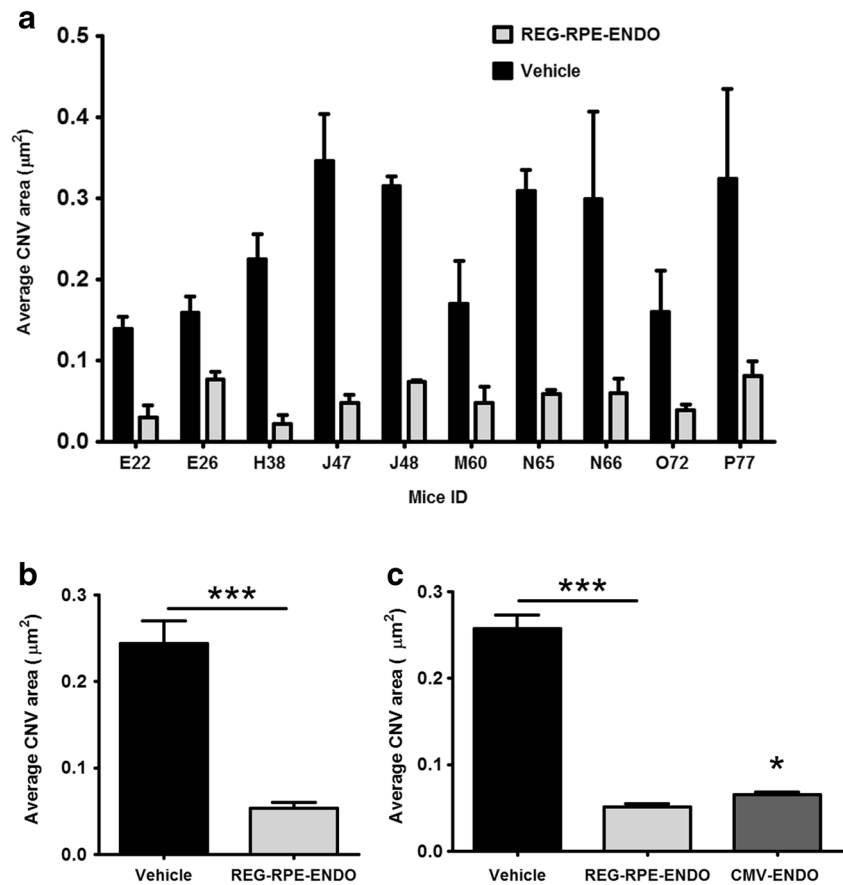
Fig. 2 Impact on CNV lesion in response to regulated gene therapy. Representative confocal micrographs of CNV lesions from RPE flat mounts subretinally injected with vehicle (top row), scAAV2-HRSE-HRE-RPE65-Endostatin (REG-RPE-ENDO; middle row), or scAAV2-CMV-Endostatin (CMV-ENDO; bottom row). Arrows indicate CNV lesion boundaries. Green = fluorescein-conjugated tomato lectin perfused vasculature; blue = DAPI nuclear stain. Scale bars = 100 μm . Twelve lesions were analyzed per experimental condition

REG-RPE-ENDO by comparison to vehicle treatment in laser-injured eyes. We further compared mean CNV area in eyes receiving either vehicle, or regulated REG-RPE-ENDO or constitutively expressed CMV-ENDO. The results of these experiments show a substantially lower level of neovascularization afforded by injection of either REG-ENDO or CMV-ENDO gene therapy than with vehicle alone (Fig. 3c). The mean CNV area in eyes treated with the CMV-ENDO vector was 76% smaller than that in the vehicle controls ($P < 0.001$), and the CNV areas in eyes treated with regulated and unregulated vectors were not significantly different (Fig. 3c).

SD-OCT imaging of laser-induced lesions

Spectral domain optical coherence tomography (SD-OCT) is a well-established method for measuring the clinical progression of AMD [32]. In addition, this imaging modality is very effective for measuring volume of CNV lesions induced by laser injury in mice [33]. We employed SD-OCT to assess the impact of regulated gene therapy in our model of CNV. Mice were first administered gene therapy or vehicle by subretinal injection and then 14 days later subjected to laser treatment. At the 14th day post-laser time point, we employed SD-OCT to quantify retinal CNV lesion volume. Comparison of SD-OCT images of the CNV volume in a representative vehicle-injected eye (Fig. 4a) with that in a REG-RPE-ENDO-treated eye (Fig. 4b) illustrates the reduced CNV volume in

Fig. 3 Regulated endostatin production reduced the size of CNV lesions. **a** Each set of bar graphs represents the average areas of CNV lesions in eyes treated with REG-RPE-ENDO or vehicle with the mouse designation (letter and number is given below). ($*P < 0.001$, *t* test). **b** Mean CNV area for REG-RPE-ENDO-injected (gray bars) and contralateral, vehicle-injected eyes (black bars) from the same mouse ($n = 10$ of each; $P < 0.01$). **c** Comparison of mean CNV area in all eyes treated with REG-RPE-ENDO, all eyes treated with CMV-ENDO and all vehicle-injected eyes (vehicle 53 lesions; REG-RPE-ENDO 53 lesions; CMV-ENDO 17 lesions; $***P < 0.01$; * differs from vehicle alone with $P < 0.01$)



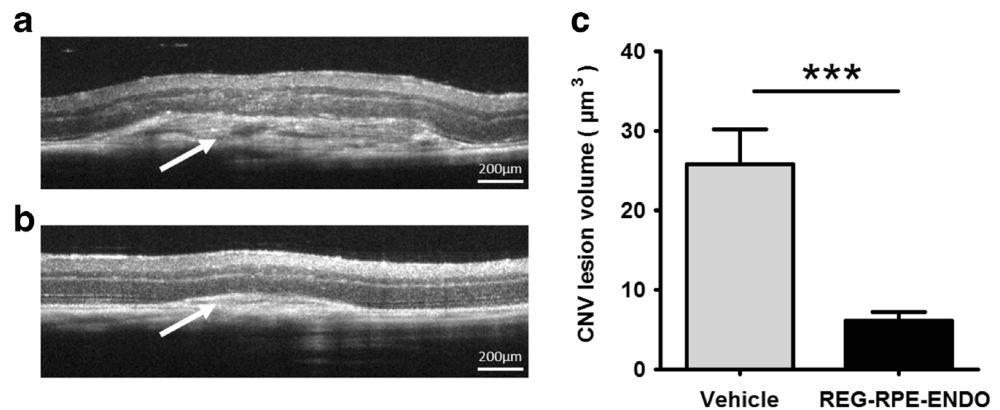
the latter. Six lesions were measure from vehicle-treated eyes and nine lesions were measured from REG-RPE-ENDO-treated eyes. SD-OCT images of CNV lesions showed significantly decreased neovascularization volume in animals receiving REG-RPE-ENDO by comparison to animals receiving vehicle injection alone (Fig. 4c).

Regulated expression of endostatin mRNA

Measurement of endostatin mRNA was conducted on RPE-choroid from laser-injured mice that had received either gene therapy or vehicle alone. The number of mice employed for

mRNA analysis is indicated in the figure legend. Injection of REG-RPE-ENDO did not lead to elevation of endostatin mRNA in the RPE/choroid detected by qRT-PCR in the absence of laser treatment at 21 days (Fig. 5a) following subretinal injection of vector. However, laser treatment at 21 days after REG-RPE-ENDO vector administration resulted in significantly elevated endostatin mRNA levels at 3, 7, and 14 days post-laser (Fig. 5b) compared to pre-laser levels. Endostatin mRNA levels returned to baseline (pre-laser) levels by 45 days after laser injury (differing significantly from 14-day post-laser time point; $P < 0.01$). The eyes examined by qRT-PCR even 120 days after injection of REG-RPE-

Fig. 4 SD-OCT images of laser-induced CNV lesions. Representative image showing the horizontal plane of OCT imaging of eyes injected with vehicle (**a**) or REG-RPE-ENDO (**b**) 14 days post-laser. The white arrow in each image indicates the laser-induced lesion. The graph shows mean CNV volume (**c**) of the isolated lesions from the eyes treated with REG-RPE-ENDO ($n = 9$ lesions) and vehicle ($n = 6$)-injected eyes ($***P < 0.001$; unpaired *t* test)



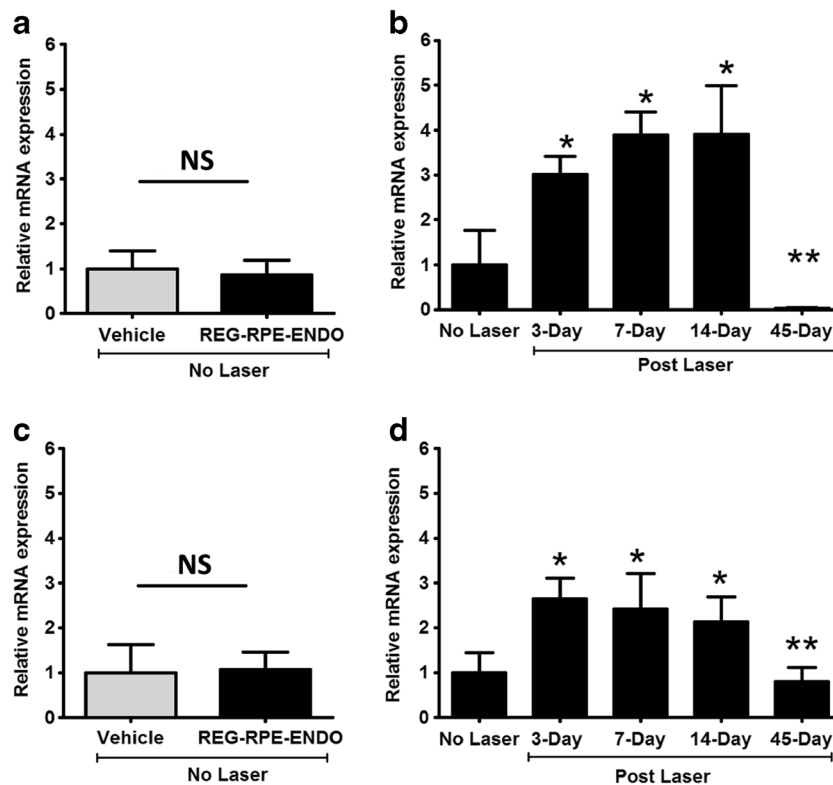


Fig. 5 Regulated expression of endostatin mRNA in RPE/choroid measured by quantitative PCR. The bar graphs represent the relative mRNA levels measured by quantitative real-time PCR as described in the “Methods” section. All values were normalized to sham-injected eyes not subjected to laser injury. Relative gene expression was quantified by comparison to mRNA levels for the housekeeping gene encoding GAPDH. **a** Comparison of REG-RPE-ENDO and vehicle-injected eyes at 21 days after subretinal injection with no subsequent laser injury. **b** Levels of endostatin mRNA in eyes injected with RPE-REG-ENDO at

3 days ($n = 5$), 7 days ($n = 5$), and 14 days ($n = 6$) following laser injury (* differs from no laser control with $P < 0.05$; ** differs from 14 days post-laser with $P < 0.01$). **c** Levels of endostatin mRNA in eyes injected with REG-RPE-ENDO without laser injury, compared to vehicle-injected eyes 4 months after subretinal injection. **d** Levels of endostatin mRNA in eyes injected with REG-RPE-ENDO at increasing intervals following laser injury that was performed 4 months following subretinal injection (* differs from no laser control with $P < 0.05$; ** differs from 14 days post-laser with $P < 0.01$)

ENDO still showed no elevation of endostatin mRNA in the RPE/choroid (Fig. 5c). However, laser treatment 120 days after vector administration resulted in significantly elevated endostatin mRNA levels at 3, 7, and 14 days post-laser (Fig. 5d) compared to pre-laser levels. Again at 45 days following laser treatment, levels of mRNA had fallen significantly below the levels measured at the 14-day post-laser time point ($P < 0.01$).

Regulated expression of endostatin protein

Endostatin levels measured by ELISA (Fig. 6) showed induced expression of endostatin at 5 days post-laser and the level was sustained until 14 days post-laser in vector-treated eyes compared to either vehicle-injected eyes treated with laser or to vector-injected eyes that were not treated with laser. Three days post-laser injury, a high level of human endostatin protein was localized in the area of laser damage (Fig. 7). Furthermore, endostatin was localized at the RPE/choroid interface, indicating its production from the basal RPE. No detectable endostatin was observed in non-lasered eyes treated

with REG-RPE-ENDO (data not shown). Enhanced endostatin was expressed in laser-treated retinas injected with REG-RPE-ENDO vector compared to vehicle-treated retinas (Fig. 7). The low-level background staining seen in these eyes and in vehicle-injected lesions is most likely due to some cross-reactivity of the antibody to endogenous mouse endostatin/collagen XVIII around Bruch’s membrane and the inner limiting membrane.

Discussion

We report the successful suppression of CNV by an RPE-specific, hypoxia-regulated vector. We previously reported that our hypoxia-regulated, RPE-specific promoter is effectively silenced in normoxic RPE cells in vitro, not activated in non-RPE cells, and dramatically induced in hypoxic RPE cells [18]. These in vivo results demonstrate that areas of CNV lesions were significantly and equivalently reduced by treatment with either unregulated (CMV-ENDO) or the regulated (REG-RPE-ENDO) vectors.

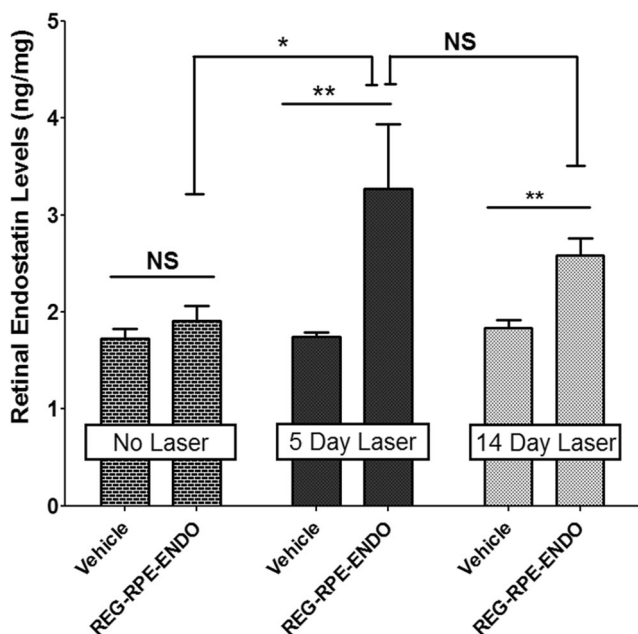


Fig. 6 Induced expression of regulated endostatin following laser injury. The histograms indicate the level of endostatin (ng per mg protein) measured by ELISA in eyes treated with REG-RPE-ENDO or with vehicle either without laser treatment at 5 days or 24 days post-laser treatment. $N=5$ in each case. * $P<0.05$ and ** $P<0.01$; NS not significant

An ideal therapeutic approach for the treatment of wet AMD would inhibit or reverse oxidative stress, inflammatory cytokine production, and neovascularization in the posterior retina. Concerns regarding engineering a gene therapy vector

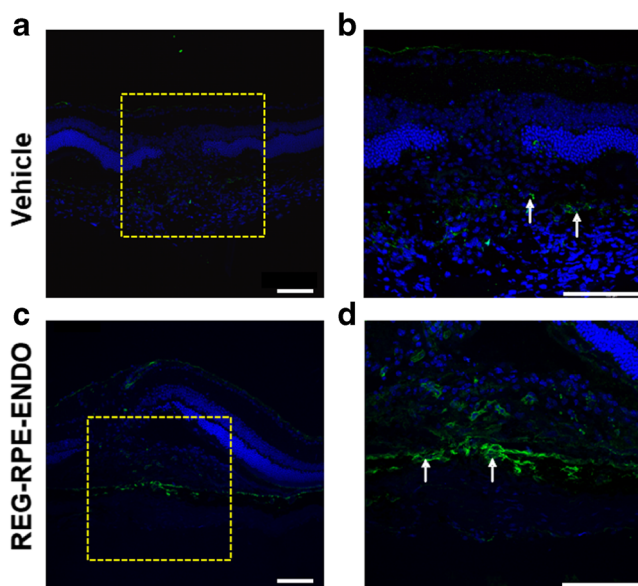


Fig. 7 Endostatin immunofluorescence. Immunofluorescence localization of human endostatin (green) in cryosections of CNV lesions in eyes injected with vehicle (**a, b**) or regulated endostatin (**c, d**) and harvested 3 days post-laser injury. **b** and **d** are higher magnification images of **a** and **c**. Arrows indicate RPE/choroid interface. Scale bars = 100 μm . Six eyes were analyzed per experimental condition

to inhibit neovascularization include how much or how often the transgene product should be produced. The options are constitutive or regulated production of the gene therapy effector protein, and the cell specificity of expression of the therapeutic protein. Constitutive expression of anti-inflammatory agents has reduced arthritis [34], and constitutive production of anti-apoptotic agents have been shown to protect the brain [35], cardiovascular system [36], and retina [37, 38]. Takahashi et al. demonstrated that constitutive expression of endostatin in the mouse eye attenuated VEGF-induced vascular leakage, neovascularization, and retinal detachment [39]. While constitutive expression may seem promising, the potential for damage to retinas continuously exposed to high levels of endostatin cannot be ignored. For example, in non-diseased regions of the eye, elevated endostatin could interfere with the neurotrophic effects of VEGF on photoreceptors and alter retinal organization [40, 41], or induce atrophy or reduce fenestrations of the choriocapillaris [42] which is dependent on VEGF from the RPE [43]. By using a regulated vector, only hypoxic foci where neovascularization starts would be exposed to high levels of endostatin. In the retina of AMD patients, foci with low levels of oxygen can be observed. Using our therapy, these pockets could be sites of continuous endostatin production. Our data in this mouse model suggest that REG-RPE-ENDO vector will supply sufficient endostatin in the vicinity of neovascular lesions to attenuate choroidal neovascularization.

Tissue-specific promoters offer additional regulation that reduces transgene expression in non-target cells, and thereby help to minimize damaging effects of vector-based expression in the surrounding healthy tissue [44–46]. Cell-specific promoters for RPE cells include the RPE65 promoter and the VMD2 promoter which have been previously incorporated into gene transfer vectors [45, 47]. Our results are consistent with earlier studies indicating that experimentally induced CNV can be efficiently inhibited by angiostatic peptides expressed specifically by the RPE [21, 48]. Previous studies have demonstrated that SD-OCT in animal models enables the investigator to perform measurement of CNV volume with a level of accuracy that is equivalent to that achieved in morphometric analysis of histological sections and to apply this technique effectively to analysis of relevant pathological processes [49]. Using SD-OCT, we demonstrated that eyes treated with REG-RPE-ENDO had significantly smaller CNV volumes than did contralateral vehicle-treated eyes.

Hypoxia-regulated gene therapy has been proposed as an expression strategy for cancer, cardiovascular disease, retinal diseases, and other ischemic disorders. The regulatory elements conferring hypoxia regulation are primarily HIF-1 binding sites, which have been identified and characterized. Investigations with hypoxia-regulated vectors have promoted their potential application for ischemic diseases and cancer [50]. Addressing retinal disease, Bainbridge et al. demonstrated that incorporation

of multiple copies of the HRE into a promoter resulted in significantly enhanced GFP expression in areas of laser-induced hypoxia in the mouse model of CNV [51], although their HRE-enhanced promoter continued to exhibit considerable activity in normoxia. This result may be explained by either leaky basal expression or additional normoxic regulators in the HIF-1 pathway. In particular, by employing a vector with HRE domains plus a proximal SV40 promoter sequence, Bainbridge et al. detected GFP transgene expression in only a few photoreceptors prior to laser treatment [51]. While the promoter in their vector is not cell-type specific, the result points to the potential for leaky basal expression in normoxia that is elicited through the contribution of a minimal proximal promoter domain. Alternatively, mild oxidative or inflammatory signaling could potentially have elicited some HIF signaling to activate their therapy.

Ideally, a hypoxia-regulated gene therapy vector should both drive enhanced expression in hypoxia and remain minimally active in normoxia. The greater suppression in normoxia observed in the present study most likely derives from the incorporation into the promoter of silencer elements designed by Webster et al. They developed an elegant solution to silencing hypoxia-regulated gene expression by creating a cassette that included multiple copies of the HRE and neuronal silencer elements (NRSE) that inactivated transgene expression in tissues other than the target cell type [18, 52, 53]. In this construct, it is likely that the binding of HIF-1 to the HRE displaces the trans-acting silencing factor. Our vector employs this additional regulatory element to reduce basal activity of the promoter in normoxia. In applications for retinal disease, we previously reported that the hypoxia responsiveness of our promoter was further enhanced by the addition of six hypoxia responsive elements to the promoter [18].

The *RPE65* and the vitelliform macular dystrophy (*VMD2*) promoters have been used to deliver anti-angiogenic agents with an RPE cell-specific expression pattern. Balagán et al. used a portion of the *VMD2* promoter for RPE cell-specific delivery of endostatin and angiostatin by lentiviral vectors and obtained a significant reduction of both neovascularization and vascular hyperpermeability in experimental CNV [24]. Campochiaro and collaborators [48] used EIAV-mediated co-delivery of endostatin and angiostatin with the *VMD2* RPE-specific promoter to yield significant reduction in CNV in the mouse model with expression of the transgene limited to RPE. Although the *RPE65* promoter has been used for RPE cell-specific gene therapy [54], the experiments reported here represent the first use of *RPE65* as a promoter in hypoxia-regulated anti-angiogenic gene therapy. In the present study, the vector was specifically regulated by hypoxia responsive domains and RPE-specific promoter domains respectively which were previously shown individually to be capable of regulating gene expression in the retina in vivo [22, 26].

The timing of in vivo expression from the HIF-1-regulated vector is very important since the goal is to initiate treatment that coincides with disease onset. In the murine model of laser-induced CNV, increasing levels of HIF-1 are localized within the lesion at the level of the RPE, with high levels at 3 days post-laser injury [55, 56], a decline at day 7, and returning to baseline by day 14; VEGF expression in the same area peaked at day 7 and remained elevated through day 14 (the last time point observed) [55]. The HIF (HIF-1-alpha and/or HIF-1-beta) transcription factor in retina is, to a large extent, expressed in a parallel fashion between the mouse CNV model and clinical observations in neovascular AMD (nAMD) [57]. In human CNV membranes from AMD patients, HIF-2-alpha was generally strongly expressed and HIF-1-alpha was weakly positive [5]. Notably, HIF expression did not co-localize with endothelial cells in human samples. Overall, the human AMD and mouse data suggested the choroidal vasculature was responding to hypoxia in the surrounding tissue [5, 57].

In a recent clinical trial, a siRNA designed to target VEGF used in combination with ranibizumab was found to be efficacious but there was still the necessity for multiple injections of the therapy [58]. Anti-VEGF miRNAs in combination with expression of PEDF has been tested in mouse models using lentivirus. Such miRNAs may be advantageous over synthetic siRNA because they already perform anti-VEGF functions endogenously in the retina [59]. The recent lentivirus trial expressing endostatin and angiostatin showed a dose-related increase in aqueous humor levels of endostatin and angiostatin [25]. There was an apparent reduction in fluorescein angiographic leakage corresponding to expression levels. However, only one subject may have had possible anti-permeability activity. Importantly, the Lentivirus trial involved patients with advanced nAMD with irreversible subretinal fibrosis but the strategy was not yet employed in early-stage nAMD. Our hypoxia-regulated and RPE-specific vector may be more effective for targeting vessels as conditions arise to induce vessel growth rather than after neovascularization is established. Key studies on endostatin's therapeutic efficacy point to the greatest anti-angiogenic effect of endostatin on early-stage disease [60]. A further factor in eliciting therapeutic efficacy has been reported to involve achieving a dose of endostatin within a critical range for inhibition of neovascularization [61]. Our regulated transgene expression may be more effective than constitutive expression for achieving such an optimal endostatin concentration.

We have confirmed high-level endostatin mRNA expression at 3 days, 7 days, and 14 days after laser treatment delivered at either 21 days or 120 days post-injection. While in one study [56] global HIF-1 levels were reported to be extinguished by day 14, our current data on continued REG-RPE-ENDO at 14 days post-laser is likely to reflect activity from hypoxic multicellular pockets in the microenvironment

of the laser lesions where sufficient HIF-1 may still be capable of inducing endostatin transgene expression.

An important benefit of our pathology-initiated, site-specific therapeutic platform is potential for prophylactic application. Currently available therapies are administered after vessel growth is advanced, often after significant damage to the retina has occurred, and needs to be re-administered when CNV recurs. Current diagnostic tools, together with genetic predisposition, can only predict the likelihood of disease onset. Our data indicate that the REG-RPE-ENDO can be administered at least 4 months prior to the onset of the pathology and still be pathology-initiated and therapeutic. This treatment option would overcome the clinical question of when to administer therapy to people with high risk of developing AMD, would reduce the need for frequent clinical checkups in patients at high risk for CNV, and may prevent or reduce recurrence of the CNV, with substantial economic impact on health care.

Acknowledgements We thank Eleut Hernandez, Bascom Palmer Eye Institute, University of Miami, Miller School of Medicine, for the help in experiments on the mouse model of choroidal neovascularization.

Funding This research was supported by NIH grant EYO16119 (JCB), NIH Core grant P30EY014801 (ASL), Research Priority grant from FAU (JCB), Davimos Family Endowment for Excellence in Science (JCB), American Heart Association grant 0815022E (MRB), and NIH grant 1K99EY027013 [MRB].

References

- Friedman DS, O'Colmain BJ, Munoz B et al (2004) Prevalence of age-related macular degeneration in the United States. *Arch Ophthalmol* 122:564–572
- Vitale S, Clemons TE, Agron E et al (2016) Evaluating the validity of the age-related eye disease study grading scale for age-related macular degeneration: AREDS2 report 10. *JAMA Ophthalmol* 134:1041–1047
- Sunness JS, Gonzalez-Baron J, Applegate CA, Bressler NM, Tian Y, Hawkins B, Barron Y, Bergman A (1999) Enlargement of atrophy and visual acuity loss in the geographic atrophy form of age-related macular degeneration. *Ophthalmology* 106:1768–1779
- Ishikawa K, Kannan R, Hinton DR (2016) Molecular mechanisms of subretinal fibrosis in age-related macular degeneration. *Exp Eye Res* 142:19–25
- Sheridan CM, Pate S, Hiscott P, Wong D, Pattwell DM, Kent D (2009) Expression of hypoxia-inducible factor-1alpha and -2alpha in human choroidal neovascular membranes. *Graefes Arch Clin Exp Ophthalmol* 247:1361–1367
- Campochiaro PA, Aiello LP, Rosenfeld PJ (2016) Anti-vascular endothelial growth factor agents in the treatment of retinal disease: from bench to bedside. *Ophthalmology* 123:S78–S88
- Villegas VM, Aranguren LA, Kovach JL, Schwartz SG, Flynn HW Jr (2017) Current advances in the treatment of neovascular age-related macular degeneration. *Expert Opin Drug Deliv* 14:273–282
- Williams T, Reeves BC, Foss AJ, Fell G (2012) Risks of adverse events with therapies for age-related macular degeneration: a response. *Arch Ophthalmol* 130:124–125 author reply 125–126
- Martin DF, Maguire MG, Ying GS, Grunwald JE, Fine SL, Jaffe GJ (2011) Ranibizumab and bevacizumab for neovascular age-related macular degeneration. *N Engl J Med* 364:1897–1908
- Nishijima K, Ng YS, Zhong L, Bradley J, Schubert W, Jo N, Akita J, Samuelsson SJ, Robinson GS, Adamis AP, Shima DT (2007) Vascular endothelial growth factor-A is a survival factor for retinal neurons and a critical neuroprotectant during the adaptive response to ischemic injury. *Am J Pathol* 171:53–67
- Semenza GL (2014) Oxygen sensing, hypoxia-inducible factors, and disease pathophysiology. *Annu Rev Pathol* 9:47–71
- Hellwig-Burgel T, Rutkowski K, Metzen E, Fandrey J, Jelkmann W (1999) Interleukin-1beta and tumor necrosis factor-alpha stimulate DNA binding of hypoxia-inducible factor-1. *Blood* 94:1561–1567
- Semenza GL, Agani F, Booth G, Forsythe J, Iyer N, Jiang BH, Leung S, Roe R, Wiener C, Yu A (1997) Structural and functional analysis of hypoxia-inducible factor 1. *Kidney Int* 51:553–555
- Campochiaro PA (2013) Ocular neovascularization. *J Mol Med (Berl)* 91:311–321
- Iwase T, Fu J, Yoshida T, Muramatsu D, Miki A, Hashida N, Lu L, Oveson B, Lima e Silva R, Seidel C, Yang M, Connelly S, Shen J, Han B, Wu M, Semenza GL, Hanes J, Campochiaro PA (2013) Sustained delivery of a HIF-1 antagonist for ocular neovascularization. *J Control Release* 172:625–633
- Lin M, Hu Y, Chen Y, Zhou KK, Jin J, Zhu M, le YZ, Ge J, Ma JX (2012) Impacts of hypoxia-inducible factor-1 knockout in the retinal pigment epithelium on choroidal neovascularization. *Invest Ophthalmol Vis Sci* 53:6197–6206
- Zhang C, Wang YS, Wu H et al (2010) Inhibitory efficacy of hypoxia-inducible factor 1alpha short hairpin RNA plasmid DNA-loaded poly (D, L-lactide-co-glycolide) nanoparticles on choroidal neovascularization in a laser-induced rat model. *Gene Ther* 17:338–351
- Dougherty CJ, Smith GW, Dorey CK, Prentice HM, Webster KA, Blanks JC (2008) Robust hypoxia-selective regulation of a retinal pigment epithelium-specific adeno-associated virus vector. *Mol Vis* 14:471–480
- Prentice HM, Biswal MR, Dorey CK, Blanks JC (2011) Hypoxia-regulated retinal glial cell-specific promoter for potential gene therapy in disease. *Invest Ophthalmol Vis Sci* 52:8562–8570
- O'Reilly MS, Boehm T, Shing Y, Fukai N, Vasios G, Lane WS, Flynn E, Birkhead JR, Olsen BR, Folkman J (1997) Endostatin: an endogenous inhibitor of angiogenesis and tumor growth. *Cell* 88:277–285
- Mori K, Ando A, Gehlbach P, Nesbitt D, Takahashi K, Goldstein D, Penn M, Chen CT, Mori K, Melia M, Phipps S, Moffat D, Brazzell K, Liao G, Dixon KH, Campochiaro PA (2001) Inhibition of choroidal neovascularization by intravenous injection of adenoviral vectors expressing secreted endostatin. *Am J Pathol* 159:313–320
- Biswal MR, Prentice HM, Dorey CK, Blanks JC (2014) A hypoxia-responsive glial cell-specific gene therapy vector for targeting retinal neovascularization. *Invest Ophthalmol Vis Sci* 55:8044–8053
- Auricchio A, Behling KC, Maguire AM, O'Connor EE, Bennett J, Wilson JM, Tolentino MJ (2002) Inhibition of retinal neovascularization by intraocular viral-mediated delivery of anti-angiogenic agents. *Mol Ther* 6:490–494
- Balaggan KS, Binley K, Esapa M, MacLaren RE, Iqbal S, Duran Y, Pearson RA, Kan O, Barker SE, Smith AJ, Bainbridge JW, Naylor S, Ali RR (2006) ELAV vector-mediated delivery of endostatin or angiostatin inhibits angiogenesis and vascular hyperpermeability in experimental CNV. *Gene Ther* 13:1153–1165
- Campochiaro PA, Lauer AK, Sohn EH, Mir TA, Naylor S, Anderton MC, Kelleher M, Harrop R, Ellis S, Mitrophanous KA (2017) Lentiviral vector gene transfer of endostatin/angiostatin for macular degeneration (GEM) study. *Hum Gene Ther* 28:99–111

26. Boulanger A, Liu S, Henningsgaard AA, Yu S, Redmond TM (2000) The upstream region of the Rpe65 gene confers retinal pigment epithelium-specific expression in vivo and in vitro and contains critical octamer and E-box binding sites. *J Biol Chem* 275: 31274–31282
27. Timmers AM, Zhang H, Squitieri A, Gonzalez-Pola C (2001) Subretinal injections in rodent eyes: effects on electrophysiology and histology of rat retina. *Mol Vis* 7:131–137
28. Biswal MR, Ahmed CM, Ildefonso CJ, Han P, Li H, Jivanji H, Mao H, Lewin AS (2015) Systemic treatment with a 5HT1a agonist induces anti-oxidant protection and preserves the retina from mitochondrial oxidative stress. *Exp Eye Res* 140:94–105
29. Tobe T, Ortega S, Luna JD, Ozaki H, Okamoto N, Derevanik NL, Viores SA, Basilico C, Campochiaro PA (1998) Targeted disruption of the FGF2 gene does not prevent choroidal neovascularization in a murine model. *Am J Pathol* 153:1641–1646
30. Lambert V, Lecomte J, Hansen S, Blacher S, Gonzalez MLA, Struman I, Sounni NE, Rozet E, de Tullio P, Foidart JM, Rakic JM, Noel A (2013) Laser-induced choroidal neovascularization model to study age-related macular degeneration in mice. *Nat Protoc* 8:2197–2211
31. Mao H, Seo SJ, Biswal MR et al (2014) Mitochondrial oxidative stress in the retinal pigment epithelium leads to localized retinal degeneration. *Invest Ophthalmol Vis Sci* 55:4613–4627
32. Sulaiman RS, Quigley J, Qi X, O'Hare MN, Grant MB, Boulton ME, Corson TW (2015) A simple optical coherence tomography quantification method for choroidal neovascularization. *J Ocul Pharmacol Ther* 31:447–454
33. Kong F, Li W, Li X, Zheng Q, Dai X, Zhou X, Boye SL, Hauswirth WW, Qu J, Pang JJ (2010) Self-complementary AAV5 vector facilitates quicker transgene expression in photoreceptor and retinal pigment epithelial cells of normal mouse. *Exp Eye Res* 90:546–554
34. Khoury M, Adriaansen J, Vervoordeldonk MJ et al (2007) Inflammation-inducible anti-TNF gene expression mediated by intra-articular injection of serotype 5 adeno-associated virus reduces arthritis. *J Gene Med* 9:596–604
35. Roy M, Hom JJ, Sapolsky RM (2002) HSV-mediated delivery of virally derived anti-apoptotic genes protects the rat hippocampus from damage following excitotoxicity, but not metabolic disruption. *Gene Ther* 9:214–219
36. Zhao J, Bolton EM, Bradley JA, Lever AM (2009) Lentiviral-mediated overexpression of Bcl-xL protects primary endothelial cells from ischemia/reperfusion injury-induced apoptosis. *J Heart Lung Transplant* 28:936–943
37. Schuetttauf F, Vorwerk C, Naskar R, Orlin A, Quinto K, Zurakowski D, Dejneka NS, Klein RL, Meyer EM, Bennett J (2004) Adeno-associated viruses containing bFGF or BDNF are neuroprotective against excitotoxicity. *Curr Eye Res* 29:379–386
38. Wu WC, Lai CC, Chen SL, Sun MH, Xiao X, Chen TL, Tsai RJ, Kuo SW, Tsao YP (2004) GDNF gene therapy attenuates retinal ischemic injuries in rats. *Mol Vis* 10:93–102
39. Takahashi K, Saishin Y, Silva RL et al (2003) Intraocular expression of endostatin reduces VEGF-induced retinal vascular permeability, neovascularization, and retinal detachment. *FASEB J* 17: 896–898
40. Ishida S, Usui T, Yamashiro K, Kaji Y, Amano S, Ogura Y, Hida T, Oguchi Y, Ambati J, Miller JW, Gragoudas ES, Ng YS, D'Amore PA, Shima DT, Adamis AP (2003) VEGF164-mediated inflammation is required for pathological, but not physiological, ischemia-induced retinal neovascularization. *J Exp Med* 198:483–489
41. Saint-Geniez M, Maharaj AS, Walshe TE et al (2008) Endogenous VEGF is required for visual function: evidence for a survival role on muller cells and photoreceptors. *PLoS One* 3:e3554
42. Kamba T, Tam BY, Hashizume H et al (2006) VEGF-dependent plasticity of fenestrated capillaries in the normal adult microvasculature. *Am J Physiol Heart Circ Physiol* 290:H560–H576
43. Saint-Geniez M, Kurihara T, Sekiyama E, Maldonado AE, D'Amore PA (2009) An essential role for RPE-derived soluble VEGF in the maintenance of the choriocapillaris. *Proc Natl Acad Sci U S A* 106:18751–18756
44. Berry M, Barrett L, Seymour L, Baird A, Logan A (2001) Gene therapy for central nervous system repair. *Curr Opin Mol Ther* 3: 338–349
45. Esumi N, Oshima Y, Li Y, Campochiaro PA, Zack DJ (2004) Analysis of the VMD2 promoter and implication of E-box binding factors in its regulation. *J Biol Chem* 279:19064–19073
46. Schon C, Biel M, Michalakis S (2015) Retinal gene delivery by adeno-associated virus (AAV) vectors: strategies and applications. *Eur J Pharm Biopharm* 95:343–352
47. Nicoletti A, Kawase K, Thompson DA (1998) Promoter analysis of RPE65, the gene encoding a 61-kDa retinal pigment epithelium-specific protein. *Invest Ophthalmol Vis Sci* 39:637–644
48. Kachi S, Binley K, Yokoi K, Umeda N, Akiyama H, Muramatsu D, Iqbal S, Kan O, Naylor S, Campochiaro PA (2009) Equine infectious anemia viral vector-mediated codelivery of endostatin and angiostatin driven by retinal pigmented epithelium-specific VMD2 promoter inhibits choroidal neovascularization. *Hum Gene Ther* 20:31–39
49. Berger A, Cavallero S, Dominguez E, Barbe P, Simonutti M, Sahel JA, Sennlaub F, Raoul W, Paques M, Bemelmans AP (2014) Spectral-domain optical coherence tomography of the rodent eye: highlighting layers of the outer retina using signal averaging and comparison with histology. *PLoS One* 9:e96494
50. Binley K, Iqbal S, Kingsman A, Kingsman S, Naylor S (1999) An adenoviral vector regulated by hypoxia for the treatment of ischaemic disease and cancer. *Gene Ther* 6:1721–1727
51. Bainbridge JW, Mistry A, Binley K et al (2003) Hypoxia-regulated transgene expression in experimental retinal and choroidal neovascularization. *Gene Ther* 10:1049–1054
52. Schoenherr CJ, Anderson DJ (1995) The neuron-restrictive silencer factor (NRSF): a coordinate repressor of multiple neuron-specific genes. *Science* 267:1360–1363
53. Webster KA, Discher DJ, Hernandez OM, Yamashita K, Bishopric NH (2000) A glycolytic pathway to apoptosis of hypoxic cardiac myocytes. Molecular pathways of increased acid production. *Adv Exp Med Biol* 475:161–175
54. Acland GM, Aguirre GD, Bennett J, Aleman TS, Cideciyan AV, Bencicelli J, Dejneka NS, Pearce-Kelling SE, Maguire AM, Palczewski K, Hauswirth WW, Jacobson SG (2005) Long-term restoration of rod and cone vision by single dose rAAV-mediated gene transfer to the retina in a canine model of childhood blindness. *Mol Ther* 12:1072–1082
55. Yang XM, Wang YS, Zhang J, Li Y, Xu JF, Zhu J, Zhao W, Chu DK, Wiedemann P (2009) Role of PI3K/Akt and MEK/ERK in mediating hypoxia-induced expression of HIF-1alpha and VEGF in laser-induced rat choroidal neovascularization. *Invest Ophthalmol Vis Sci* 50:1873–1879
56. Zhang P, Wang Y, Hui Y, Hu D, Wang H, Zhou J, du H (2007) Inhibition of VEGF expression by targeting HIF-1 alpha with small interference RNA in human RPE cells. *Ophthalmologica* 221:411–417
57. Andre H, Tunik S, Aronsson M, Kvanta A (2015) Hypoxia-inducible factor-1alpha is associated with sprouting angiogenesis in the murine laser-induced choroidal neovascularization model. *Invest Ophthalmol Vis Sci* 56:6591–6604
58. Nguyen QD, Schachar RA, Nduaka CI, Sperling M, Klammer KJ, Chi-Burris K, Yan E, Paggiarino DA, Rosenblatt I, Aitchison R, Erlich SS, MONET Clinical Study Group (2012) Evaluation of the siRNA PF-04523655 versus ranibizumab for the treatment of neovascular age-related macular degeneration (MONET Study). *Ophthalmology* 119:1867–1873

59. Askou AL, Aagaard L, Kostic C, Arsenijevic Y, Hollensen AK, Bek T, Jensen TG, Mikkelsen JG, Corydon TJ (2015) Multigenic lentiviral vectors for combined and tissue-specific expression of miRNA- and protein-based antiangiogenic factors. *Mol Ther Methods Clin Dev* 2:14064
60. Macpherson GR, Ng SS, Forbes SL, Melillo G, Karpova T, McNally J, Conrads TP, Veenstra TD, Martinez A, Cuttitta F, Price DK, Figg WD (2003) Anti-angiogenic activity of human endostatin is HIF-1-independent in vitro and sensitive to timing of treatment in a human saphenous vein assay. *Mol Cancer Ther* 2:845–854
61. Tjin Tham Sjin RM, Naspinski J, Birsner AE, Li C, Chan R, Lo KM, Gillies S, Zurakowski D, Folkman J, Samulski J, Javaherian K (2006) Endostatin therapy reveals a U-shaped curve for antitumor activity. *Cancer Gene Ther* 13:619–627